τ_0-WM: A Unified Video-Action World Model for Robotic Manipulation

Pengfei Zhou[2,*] Shengcong Chen[2,*] Di Chen[2] Jiaxu Wang[2] Rongjun Jin[2] Bingwen Zhu[1,2] Yike Pan[2] Songen Gu[2] Kuanning Wang[2] Shufeng Nan[2] Xingyu Qiu[2] Chenhao Qiu[2] Pu Yang[2] Yunuo Cai[1,2] Jianxiong Gao[2] Yifan Li[1] Yanwei Fu[1,2] Xiangyu Yue[2] Zhi Chen[2] Jianlan Luo[1,2†]

[1]Shanghai Innovation Institute [2]AGIBOT Finch

[*]Equal contribution. [†]Corresponding author.

https://tau0-wm.github.io/

arXiv:2606.01027v2 [cs.RO] 23 Aug 2026

***Abstract*—Robotic manipulation requires models that generate executable actions while anticipating and evaluating their future consequences before physical execution. We present τ_0-World Model (τ_0-WM), a unified video-action world model that integrates policy learning, video prediction, and action evaluation within a single future-predictive framework. Built on a shared video diffusion backbone, τ_0-WM provides two complementary interfaces. First, a video action model jointly predicts future visual latents and continuous action chunks from multi-view observations, language instructions, and robot state. Second, an action-conditioned video simulator rolls out candidate action chunks into multi-view futures and predicts dense task-progress scores. The model is trained on approximately $27{,}300$ hours of real-robot teleoperation, UMI-style interaction, egocentric human videos, and rollout or failure trajectories using modality-specific supervision masks. At inference time, τ_0-WM uses test-time computation to sample action candidates, rank them with re-denoising consistency, and invoke simulator-based rectification for low-quality candidates. On challenging long-horizon and fine-grained robotic manipulation tasks, τ_0-WM shows superior performance over other relevant baselines.**

I. Introduction

Robotic manipulation is fundamentally a problem of acting under uncertain physical consequences. A robot must not only infer which action is likely to satisfy a language instruction, but also anticipate how that action will change the scene through contact, object motion, and multi-step interactions. This perspective connects manipulation policies to a long line of work on predictive control and world models: a useful model should relate observations, actions, and future outcomes in a way that can improve decision making before physical execution [22, 17, 40, 41, 3]. For real robots, however, this predictive capability must be coupled with an action interface that is executable by a particular embodiment, controller, and sensing stack.

The data needed to learn these two capabilities is available in very different forms. Egocentric videos and human interaction trajectories provide broad evidence about how objects move, how contacts unfold, and how long-horizon tasks are temporally organized. Such data captures rich visual dynamics across diverse objects, scenes, and behaviors, but it does not specify actions in the control space of a deployable robot. Robot demonstrations provide precisely this grounding: they couple observations to continuous actions collected with a specific embodiment, controller, sensor suite, and action representation. Yet robot data is expensive to collect and arguably covers a much narrower subset of objects, environments, tasks. Training only on robot demonstrations yields grounded but narrow policies; training only on broad video data yields predictive but action-ungrounded models. A general manipulation system must therefore use broad interaction data without losing the executable action grounding required for deployment.

This paper studies a unified video-action world modeling formulation for robotic manipulation. The central idea is to place future observations, robot actions, and task progress within a shared predictive model, while allowing each data source to supervise only the signals it actually contains. Video-only data can train visual dynamics; robot trajectories can train executable action generation; progress and failure trajectories can train action-conditioned evaluation. In this way, heterogeneity is not treated as noise or a preprocessing inconvenience, but as a structured source of complementary supervision. The resulting representation is intended to serve not merely as an auxiliary feature for policy learning, but as an interface through which a robot can propose actions, imagine their consequences, and revise them before execution.

We present τ_0-World Model (τ_0-WM), a unified video-action framework that integrates action generation, video prediction, and action-conditioned future evaluation. Rather than separating policy learning from dynamics modeling, τ_0-WM builds both around a shared video diffusion backbone. This backbone exposes two complementary interfaces. The first is a Video Action Model (VAM), which maps multi-view observations, a language instruction, and robot state to both future visual latents and a continuous action chunk. The second is an Action-Conditioned Video Simulator (ACVS), which takes the current observation, instruction, and a candidate action chunk, and predicts the multi-view future rollout together with a dense task-progress trajectory. The distinction between these interfaces is important: VAM answers what the robot should do, while ACVS estimates what would happen if a proposed action were executed.

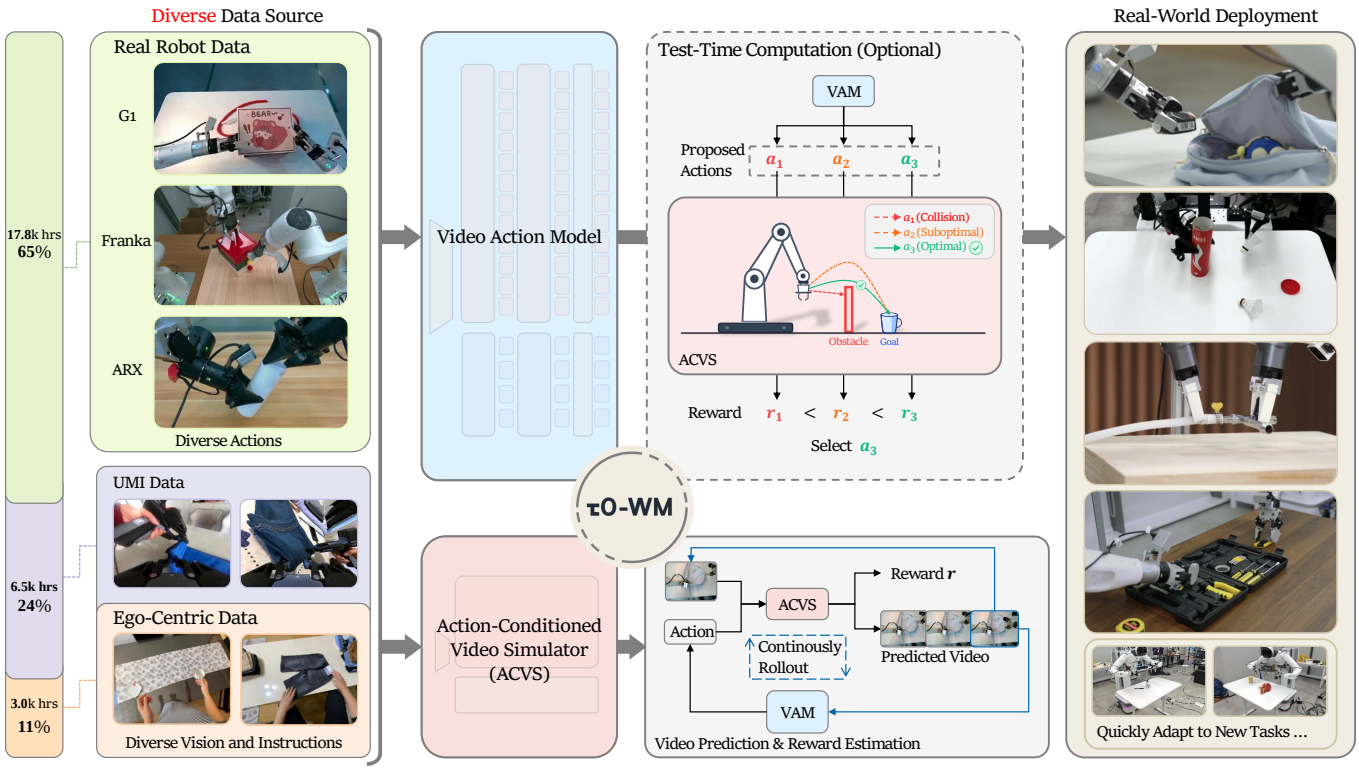

Fig. 1. **Overview of the τ_0-WM framework.** Heterogeneous interaction data from real robots, UMI-style collection, and egocentric human videos are used to train a Video Action Model and an Action-Conditioned Video Simulator. At deployment, the system proposes action candidates, evaluates imagined futures through test-time computation and simulator-based scoring, and selects or rectifies actions for robust manipulation across tasks and embodiments.

The shared predictive representation enables τ_0-WM to learn from a heterogeneous corpus of approximately 27,300 hours. This corpus includes real-robot teleoperation data, UMI-style demonstrations, egocentric human videos, and rollout or failure trajectories. These sources provide different degrees of supervision and action fidelity. Real-robot demonstrations provide deployment-aligned continuous actions; UMI-style demonstrations broaden manipulation behaviors and environments with weaker action-like signals; egocentric videos supply large-scale visual interaction dynamics without robot-compatible actions; and rollout or failure trajectories provide supervision for task progress and low-quality outcomes. We train on these sources jointly using modality-specific supervision masks, so that each sample contributes only to the losses supported by its observations, views, states, actions, and progress labels.

At inference time, this unified interface allows τ_0-WM to allocate additional computation to action selection rather than executing the first feed-forward prediction. The model first samples multiple action chunks from VAM and ranks them with a re-denoising consistency score, which measures whether a candidate is consistent with the learned conditional action distribution. When the selected candidate appears unreliable, τ_0-WM invokes ACVS to simulate the futures induced by candidate actions and estimate their task progress. The most promising imagined future is then used to condition a second VAM query, producing a refined action chunk. This yields a proposal–evaluation–revision procedure in which future prediction is used directly as a mechanism for improving robot actions before execution.

We evaluate τ_0-WM as a robot-facing system on fine-grained and long-horizon manipulation tasks across multiple embodiments. In our current evaluation, τ_0-WM achieves the best average success rate among the evaluated baselines on four manipulation tasks. Ablations further show that heterogeneous pre-training improves both zero-shot and fine-tuned performance, while test-time computation improves single-attempt execution through both re-denoising consistency selection and simulator-assisted rectification. These results support the central thesis of this work: video prediction is most useful for robotic manipulation when it is trained jointly with executable action generation and exposed at deployment time as a mechanism for imagining, scoring, and refining future outcomes.

Our contributions are threefold. First, we introduce τ_0-WM, a unified video-action world model that shares a predictive representation across policy learning and action-conditioned simulation. Second, we show how heterogeneous robot, UMI-style, egocentric, and rollout/failure data can be integrated with modality-specific supervision masks. Third, we propose a test-time proposal–evaluation–revision procedure that uses the learned world model to select and rectify actions before

execution, improving performance on challenging real-world manipulation tasks.

II. Related Work

τ_0-WM builds on two related lines of work, robotic video action models and action-conditioned video simulators, and unifies them in a single video-action world-modeling framework. We thus survey works in these two areas and their intersections.

A. Robotic Video Action Models

Video Action Models (VAMs) introduce future forecasting into robot control by jointly predicting videos and actions [29, 5, 24, 26, 45, 43, 27, 46, 28, 44]. Most recent methods build on pretrained video-generation diffusion models [39, 16, 42] and adopt a joint-denoising paradigm, where future visual latents and action chunks are generated together [1, 29, 5, 24, 26]. These works show that future prediction provides useful dynamics-aware representations for manipulation. Some recent systems further improve scalability or efficiency, such as Motus [5], which integrates understanding, video generation, world modeling, and control, and Fast-WAM [45], which studies removing future prediction during policy inference to reduce latency.

Different from prior VAMs that mainly use future prediction as an auxiliary policy-learning objective or an optional visual output, τ_0-WM treats video-action modeling as a unified foundation for manipulation. Its VAM jointly predicts multi-view future latents and executable action chunks, while sharing the same predictive representation with an action-conditioned simulator. This enables future prediction to be used not only for representation learning, but also for test-time action evaluation and rectification. Moreover, τ_0-WM is trained on heterogeneous robot, UMI, and egocentric interaction data [38, 23, 9, 31, 19], using each data source to supervise the signals it provides.

B. Action-Conditioned Video Simulators for Robotics

Another line of work uses video models as action-conditioned simulators for decision making. Early visual foresight methods learned action-conditioned video predictors and used model-predictive control to select actions whose predicted futures matched a goal [11, 10]. With recent advances in large-scale video generation [7, 14, 34, 37, 25, 39], recent robotics systems condition video models on robot actions, end-effector trajectories, or controllable tokens to predict manipulation rollouts, evaluate policies, or support reinforcement learning [1, 2, 29, 15, 21, 12, 8].

In contrast, τ_0-WM does not use the simulator as a separate module. Its Action-Conditioned Video Simulator (ACVS) shares the action interface and backbone configuration with the VAM, is trained on the same heterogeneous data mixture, and predicts both multi-view future rollouts and task-progress scores. At test time, this allows τ_0-WM to go beyond feed-forward action prediction: it samples candidate actions, ranks them by re-denoising consistency, and invokes ACVS to evaluate and rectify low-quality candidates before execution.

III. Data Sources for Predictive Robot Learning

A general-purpose Video Action Model should learn not only from a single robot embodiment or data-collection pipeline, but from heterogeneous interaction data that provides complementary forms of supervision. We therefore construct a 27.3K-hour training corpus from three sources: 17.8K hours of real-robot teleoperation on AGIBOT-G01, ARX manipulators, and dual-arm Franka systems; 6.5K hours of filtered open-source UMI-style demonstrations collected with Gen-DAS Grippers [13]; and 3.0K hours of open-source egocentric human interaction videos [19, 35, 36]. These sources differ in embodiment, viewpoint, action fidelity, collection cost, and behavioral diversity, making them naturally suited to different training objectives.

a) Real-robot teleoperation: Real-robot demonstrations provide the most reliable action supervision. In our dataset, trajectories are collected on AGIBOT-G01, ARX, and dual-arm Franka platforms across household, retail, and industrial settings, typically with a head-view camera and wrist-mounted cameras. Because these demonstrations are generated directly on robotic systems, their actions are aligned with the robot kinematics, controller interface, sensing stack, and deployment conditions. They are therefore essential for grounding the model in executable robot behavior. At the same time, real-robot data is costly to collect and limited by the available platforms, workspaces, objects, and task setups, which makes it insufficient by itself for broad generalization.

b) UMI-style demonstrations: UMI-style data offers a more scalable source of manipulation experience. By using handheld gripper-like devices, human operators can collect demonstrations in diverse environments with substantially lower infrastructure cost than full robot teleoperation. These demonstrations provide rich visual interaction data and action-like signals derived from device motion, which encode useful information about manipulation intent and object interaction. However, these signals are only weakly aligned with deployable robot actions, since the collection device differs from the target robot in embodiment, kinematics, actuation, and control interface. We therefore treat UMI-style demonstrations as scalable but weaker video-action supervision.

c) Egocentric human interaction videos: Egocentric human videos provide the broadest coverage of everyday manipulation behaviors. They expose the model to diverse objects, environments, contact patterns, state changes, and long-horizon task structure. Unlike robot or UMI data, however, egocentric videos do not contain robot-compatible action labels and differ substantially in embodiment and viewpoint. Consequently, we use them only for video prediction: they supervise visual dynamics while being excluded from action losses.

d) Unified supervision: The three sources induce a hierarchy of supervision. Real-robot data provides deployment-aligned action labels; UMI-style data provides diverse interaction trajectories with weaker action-like signals; and egocentric videos provide large-scale visual dynamics without action supervision. To train on all sources jointly, we use a unified video-action representation with modality-specific supervision

masks. For each sample, the mask specifies which inputs are observed, which targets are predicted, and which losses are active. This allows heterogeneous data to contribute to a single end-to-end objective while respecting the different reliability and availability of their supervision.

IV. Video Action Model

A. Model Interface and Problem Formulation

The Video Action Model (VAM) serves as the policy-facing interface of τ_0-WM. It jointly learns future visual dynamics and executable robot actions using a shared predictive representation. Given the current multi-view observation $\mathbf{o}_t$, language instruction $\mathbf{p}$, and robot state $\mathbf{s}_t$, VAM predicts a future latent trajectory together with an executable action chunk:

$$F_\theta(\mathbf{o}_t, \mathbf{p}, \mathbf{s}_t) \to (\hat{\mathbf{z}}_{t+1:t+H_v}, \hat{\mathbf{a}}_{t:t+H_a-1}), \tag{1}$$

where $\hat{\mathbf{z}}$ denotes future video latents over horizon H_v and $\hat{\mathbf{a}}$ denotes a continuous action chunk over horizon H_a. Future visual prediction serves not only as an auxiliary objective but also as a mechanism for learning transferable interaction dynamics from heterogeneous data sources, including videos without action annotations, while action prediction grounds the learned representation in executable robot control.

B. Architecture

As illustrated in Fig. 2 (a), VAM consists of two tightly coupled components: a video branch for future visual prediction and an action branch for executable action generation. The two branches share a common predictive representation and interact through feature-level cross-attention, allowing future visual dynamics to directly support action generation.

VAM is instantiated from Wan2.2-TI2V-5B [39]. A Wan VAE first encodes each camera view into latent tensors. For synchronized multi-view inputs, view latents are concatenated along the spatial width dimension, forming a temporally aligned latent canvas. The current observation latent is kept clean as visual context, while future latent slots are noised and denoised by the video branch. The video branch is implemented using the original Wan video DiT backbone (5B parameters) and predicts future latent trajectories through conditional denoising. The action branch is a 0.5B-parameter DiT-style action decoder [33] coupled to the video transformer. Together, they form a 5.5B-parameter Video Action Model.

At matched transformer stages, the action tokens first model temporal dependencies within the action horizon and then cross-attend to intermediate video features. These video features are conditioned on both the clean visual context and the language instruction, thereby providing the action branch with instruction-aware and dynamics-relevant visual representations. This feature-level coupling follows recent action-expert designs [29, 20], while preserving the video backbone as the shared predictive substrate.

C. Joint Flow-Matching Objective

VAM applies flow matching [30] to both future video latents and action chunks. Let $\mathbf{z} = \mathbf{z}_{t+1:t+H_v}$ and $\mathbf{a} = \mathbf{a}_{t:t+H_a-1}$ denote the training targets, and let $\mathbf{c}_t$ denote the clean encoded visual context. Given noise levels u_z and u_a, the standard flow-matching construction produces noised inputs $\tilde{\mathbf{z}}, \tilde{\mathbf{a}}$ together with velocity targets $\mathbf{v}_\mathbf{z}, \mathbf{v}_\mathbf{a}$. We optimize

$$\begin{aligned}\mathcal{L}_{\text{VAM}} = \mathbb{E}\Big[&\lambda_z \left\| f_\theta^z(\tilde{\mathbf{z}}, u_z, \mathbf{c}_t, \mathbf{p}) - \mathbf{v}_\mathbf{z} \right\|_2^2 \\ &+ \lambda_a \left\| f_\theta^a(\tilde{\mathbf{a}}, u_a, \mathbf{s}_t, \mathbf{h}) - \mathbf{v}_\mathbf{a} \right\|_2^2 \Big],\end{aligned} \tag{2}$$

where f_θ^z and f_θ^a denote the video and action vector-field heads, and $\mathbf{h}$ denotes the intermediate video features consumed by the action branch.

The expectation is taken over heterogeneous training samples with different supervision levels. Robot trajectories contribute both visual prediction and action supervision, while egocentric human videos contribute only the visual dynamics term. Missing modalities are handled through supervision masks, allowing all data sources to participate in a unified training process. In all experiments, we simply set $\lambda_z = \lambda_a = 1$.

D. Inference and Deployment

At inference time, VAM takes the latest multi-view observation $\mathbf{o}_t$, language instruction $\mathbf{p}$, and robot state $\mathbf{s}_t$ as input and predicts an executable action chunk. The future latents can be decoded into video frames when explicit visual rollouts are required, or retained as latent representations when used solely to support action generation. This enables two deployment modes. In action-only deployment, only the predicted action chunk is generated and executed in a receding-horizon manner, providing efficient real-time control. In rollout-enabled deployment, VAM additionally predicts future visual latents that can be decoded into multi-view videos, allowing future scene evolution to be explicitly visualized when desired.

V. Action-Conditioned Video Simulator

A. Simulator Interface and Problem Formulation

The Action-Conditioned Video Simulator (ACVS) serves as the evaluation interface of τ_0-WM, as illustrated in Fig. 2 (b). Whereas VAM proposes executable action chunks, ACVS estimates the future consequences induced by a candidate action. Instead of physically executing every candidate action on the robot, ACVS predicts future visual rollouts and dense reward trajectories, providing an action-conditioned proxy for deployment-time evaluation.

Given memory observations $\mathbf{o}_{t-M:t}$, a language instruction $\mathbf{p}$, and a candidate action chunk $\bar{\mathbf{a}}_{t:t+H_a-1}$, ACVS predicts future video latents together with dense reward scores:

$$G_\phi(\mathbf{o}_{t-M:t}, \mathbf{p}, \bar{\mathbf{a}}_{t:t+H_a-1}) \to (\hat{\mathbf{z}}_{t+1:t+H_v}, \hat{\mathbf{r}}_{t:t+H_a-1}), \tag{3}$$

where $\hat{\mathbf{z}}$ denotes the imagined future latent rollout and $\hat{\mathbf{r}}$ denotes the predicted reward trajectory. ACVS is not an action

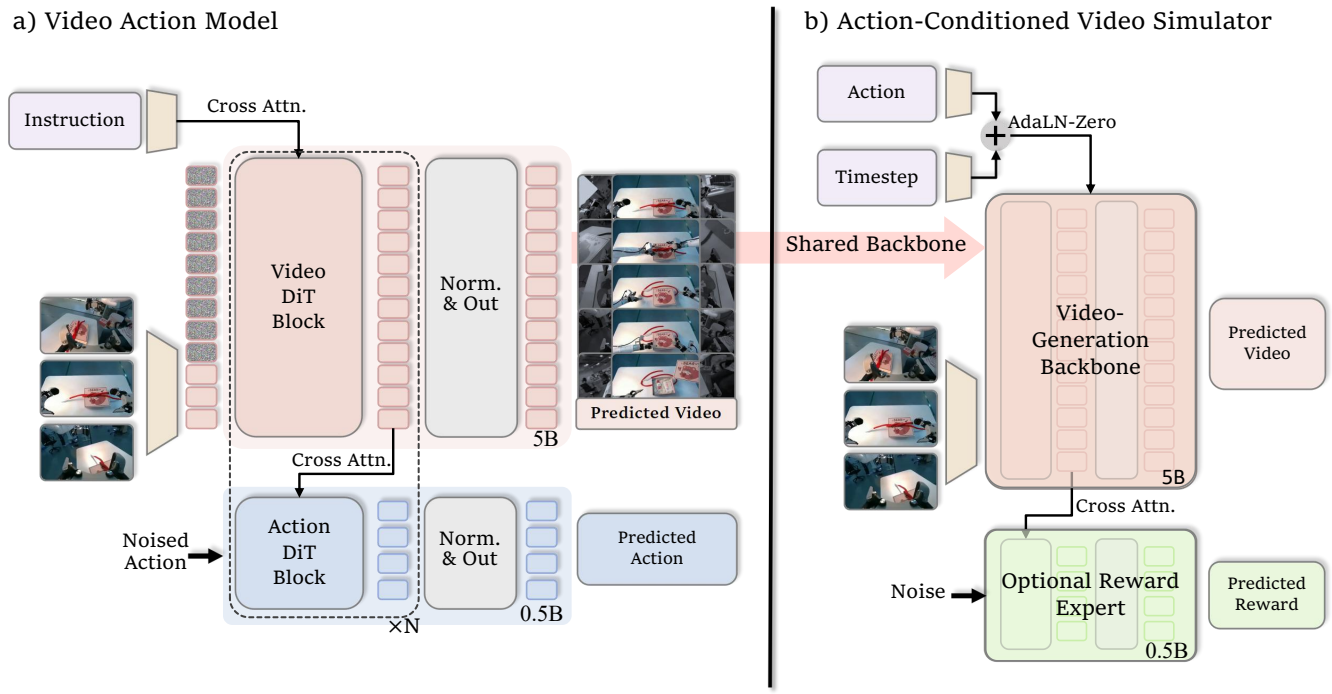

Fig. 2. **Architecture of τ_0-WM.** The Video Action Model (VAM) serves as the policy interface, jointly predicting future visual latents and executable action chunks with a shared video backbone and an Action DiT branch coupled through cross-attention. The Action-Conditioned Video Simulator (ACVS) serves as the evaluation interface, reusing the video-generation backbone to roll out VAM-proposed action chunks and predict dense reward scores for test-time action selection.

policy; it treats the candidate action chunk as a clean condition and evaluates the future it induces.

B. Architecture

ACVS reuses the Wan VAE and video transformer backbone [39] but removes the Action DiT policy branch. Memory and current observations are encoded into clean latent context, while future latent slots are initialized with noise and denoised by the video backbone.

To condition future prediction on candidate actions, we follow the action-conditioned design of Cosmos [2]. For each future latent slot ℓ, temporally aligned actions are grouped into an action block $\mathbf{b}_\ell$ and projected through lightweight MLPs:

$$\mathbf{c}_\ell^a = \psi_D(\mathbf{b}_\ell), \qquad \mathbf{m}_\ell^a = \psi_{6D}(\mathbf{b}_\ell), \tag{4}$$

which are injected into the diffusion-time embedding and AdaLN modulation embedding, respectively. The resulting action conditions are broadcast across spatial tokens and camera views for the corresponding future slot, while observation slots remain unconditioned.

Unlike VAM, ACVS does not generate actions. Its sole purpose is to estimate how the scene would evolve under a proposed action sequence, allowing different candidate actions to induce different imagined futures under the same observation and instruction.

C. Reward and Progress Scoring

In addition to predicting future visual rollouts, ACVS predicts a dense reward trajectory for each candidate action chunk. We decompose each manipulation task into subtasks and assign progress labels at the subtask level. Frame-level rewards are then estimated through Monte Carlo propagation within each subtask segment, producing dense supervision rather than a single terminal success label.

Failure data is intentionally incorporated into reward construction. For failed subtask segments, the reward is assigned a negative value across the corresponding trajectory. These failure examples teach ACVS to identify action-conditioned futures that lead to unsuccessful contact, incorrect object motion, or task regression. Consequently, ACVS learns to distinguish actions that make meaningful task progress from those that merely produce visually plausible motion.

To further improve simulator fidelity, we augment simulator training with failure-heavy and recovery trajectories. While such data may be suboptimal as direct policy supervision, it is particularly valuable for simulator learning because it exposes the model to off-distribution actions, failed interactions, and recovery behaviors that are difficult to observe from successful demonstrations alone.

D. Training Objective

ACVS uses the same flow-matching formulation as VAM and jointly supervises future video latents and dense re-

Algorithm 1 Test-Time Computation

Require: VAM F_θ, ACVS G_ϕ
Require: current context $\mathcal{C}_t$
Require: candidate budget N, threshold γ
Sample N candidate actions $\{\bar{\mathbf{a}}^{(i)}\}_{i=1}^{N}$
for $i = 1, \dots, N$ **do**
    Compute $S_{\mathrm{RCS}}^{(i)}$
end for
$i^\star \leftarrow \arg\max_i S_{\mathrm{RCS}}^{(i)}$
if $S_{\mathrm{RCS}}^{(i^\star)} \geq \gamma$ **then**
    return $\bar{\mathbf{a}}^{(i^\star)}$
end if
for $i = 1, \dots, N$ **do**
    Evaluate candidate using ACVS
    Compute rollout value $J^{(i)}$
end for
$j^\star \leftarrow \arg\max_i J^{(i)}$
return $\mathrm{LAR}(\hat{\mathbf{z}}^{(j^\star)})$

ward trajectories. Let $\mathbf{c}_{t-M:t}$ denote the clean visual context, $\mathbf{z}_{t+1:t+H_v}$ the future latent rollout induced by candidate action $\bar{\mathbf{a}}$, and $\mathbf{r}_{t:t+H_a-1}$ the target reward trajectory. Given noise levels u_z and u_r, the standard flow-matching construction produces noised inputs $\tilde{\mathbf{z}}, \tilde{\mathbf{r}}$ together with velocity targets $\mathbf{v}_{\mathbf{z}}, \mathbf{v}_{\mathbf{r}}$. We optimize

$$\begin{aligned}\mathcal{L}_{\mathrm{ACVS}} = \mathbb{E}\Big[\lambda_z \left\| g_\phi^z(\tilde{\mathbf{z}}, u_z, \mathbf{c}_{t-M:t}, \mathbf{p}, \bar{\mathbf{a}}) - \mathbf{v}_{\mathbf{z}} \right\|_2^2 \\ + \lambda_r \left\| g_\phi^r(\tilde{\mathbf{r}}, u_r, \mathbf{h}) - \mathbf{v}_{\mathbf{r}} \right\|_2^2 \Big],\end{aligned} \tag{5}$$

where g_ϕ^z and g_ϕ^r denote the video and reward velocity predictors, respectively, and $\mathbf{h}$ denotes the action-conditioned video features consumed by the reward head. In all experiments, we simply set $\lambda_z = \lambda_r = 1$.

VI. Test-Time Computation

Pre-training on large-scale heterogeneous interaction data makes the conditional action distribution inherently multimodal: for the same instruction and scene, the robot may complete the task through multiple feasible action sequences. These solutions can differ in precision, robustness, and likelihood of success. Consequently, selecting a high-quality action becomes an important deployment-time problem.

To address this challenge, τ_0-WM adopts a coarse-to-fine test-time computation strategy. It first samples multiple action candidates from VAM and applies a lightweight self-consistency filter to identify reliable candidates. Only when the sampled candidates appear unreliable does the system invoke ACVS for more expensive rollout-based evaluation and action rectification. This design preserves real-time performance in most situations while retaining the ability to recover from difficult states. The overall procedure is summarized in Alg. 1.

Algorithm 2 Low-quality Action Rectification

Require: selected rollout latent $\hat{\mathbf{z}}^{(j^\star)}$
Convert $\hat{\mathbf{z}}^{(j^\star)}$ into future conditioning
Re-query VAM with $\mathbf{o}_t, \mathbf{p}, \mathbf{s}_t$ and the selected future condition
Generate refined action chunk $\tilde{\mathbf{a}}$
return $\tilde{\mathbf{a}}$

A. Re-denoising Consistency Score

Given the current context $\mathcal{C}_t = (\mathbf{o}_t, \mathbf{p}, \mathbf{s}_t)$, VAM samples N candidate action chunks $\{\bar{\mathbf{a}}^{(i)}\}_{i=1}^{N}$.

For each candidate, we randomly sample K flow timesteps and re-noise the action according to the same flow-matching process used during training. The re-noised action is then evaluated by VAM's action vector field, producing an average re-denoising error $\mathcal{E}_{\mathrm{RCS}}^{(i)}$.

We define the Re-denoising Consistency Score (RCS) as

$$S_{\mathrm{RCS}}^{(i)} = -\mathcal{E}_{\mathrm{RCS}}^{(i)}, \tag{6}$$

and select

$$i^\star = \arg\max_i S_{\mathrm{RCS}}^{(i)}. \tag{7}$$

RCS serves as a lightweight distributional filter. It favors candidates that are more consistent with the learned conditional action manifold while introducing negligible computational overhead compared with rollout-based evaluation.

B. Low-quality Action Rectification

Although RCS identifies the most self-consistent candidate among the sampled actions, all candidates may still be poor in challenging states. We therefore introduce Low-quality Action Rectification (LAR).

When the selected candidate satisfies

$$S_{\mathrm{RCS}}^{(i^\star)} < \gamma, \tag{8}$$

where γ denotes a reliability threshold, ACVS is invoked to evaluate all candidate actions. For each candidate action chunk, ACVS predicts an imagined rollout and a dense reward trajectory

$$(\hat{\mathbf{z}}^{(i)}, \hat{\mathbf{r}}^{(i)}) = G_\phi(\mathbf{o}_{t-M:t}, \mathbf{p}, \bar{\mathbf{a}}^{(i)}). \tag{9}$$

The rollout value is computed as

$$J^{(i)} = \max_{0 \leq q < H_a} \hat{r}_{t+q}^{(i)}, \tag{10}$$

where $J^{(i)}$ measures the maximum task progress achieved by the imagined rollout. The highest-value rollout

$$j^\star = \arg\max_i J^{(i)} \tag{11}$$

is selected as the most promising future.

Fig. 3. **Illustrations of our evaluation tasks.** (a) Storing different tools on the desk into their corresponding places in the toolbox (*Toolbox*). (b) Unzipping the school bag, storing objects into it, and zipping up (*School Bag*). (c) Connecting the hose to the faucet and securing it (*Faucet*). (d) Storing the badminton shuttlecocks and closing the lid (*Badminton*).

Instead of directly executing the corresponding action, we perform a second policy query conditioned on the selected future rollout. Specifically, the rollout latent $\hat{\mathbf{z}}^{(j^\star)}$ is converted into an additional future condition and injected into VAM, allowing the policy to generate a refined action chunk that is explicitly guided toward the selected high-value future. The rectification procedure is summarized in Alg. 2.

VII. Experimental Evaluation

We evaluate τ_0-WM on long-horizon, fine-grained real-robot manipulation tasks. Our experiments aim to answer three questions: (i) whether the proposed VAM enables strong policy performance on challenging multi-stage manipulation tasks, (ii) whether heterogeneous pre-training with robot, UMI-style, and egocentric interaction data improves downstream performance, and (iii) whether deployment-time computation further improves closed-loop execution through action selection and rectification. We compare against representative policy and video-action baselines and conduct ablations on both data composition and test-time computation.

Experimental setup. Experiments span three robot embodiments—AGIBOT-G01, ARX manipulators, and a dual-arm Franka system—and include language-conditioned, multi-view packing and assembly tasks. The primary evaluation metric is task success rate. We compare τ_0-WM against representative policy and video-action baselines, including $\pi_{0.5}$ [6] and Fast-WAM [45]. For deployment-time reasoning, we additionally compare our test-time computation strategy against standard execution, classifier-free guidance (CFG) [18], and Action Coherence Guidance (ACG) [32]. Additional implementation details, including training hyperparameters, deployment latency, and inference settings, are provided in the appendix.

A. Main Results

We evaluate closed-loop execution on four precision-sensitive manipulation tasks shown in Fig. 3, all of which are excluded from the pre-training corpus. These tasks require long-horizon reasoning, multi-stage object interaction, and precise geometric alignment. For example, *School Bag* requires sequential zipper manipulation and object placement, while *Faucet* requires accurate hose alignment and secure

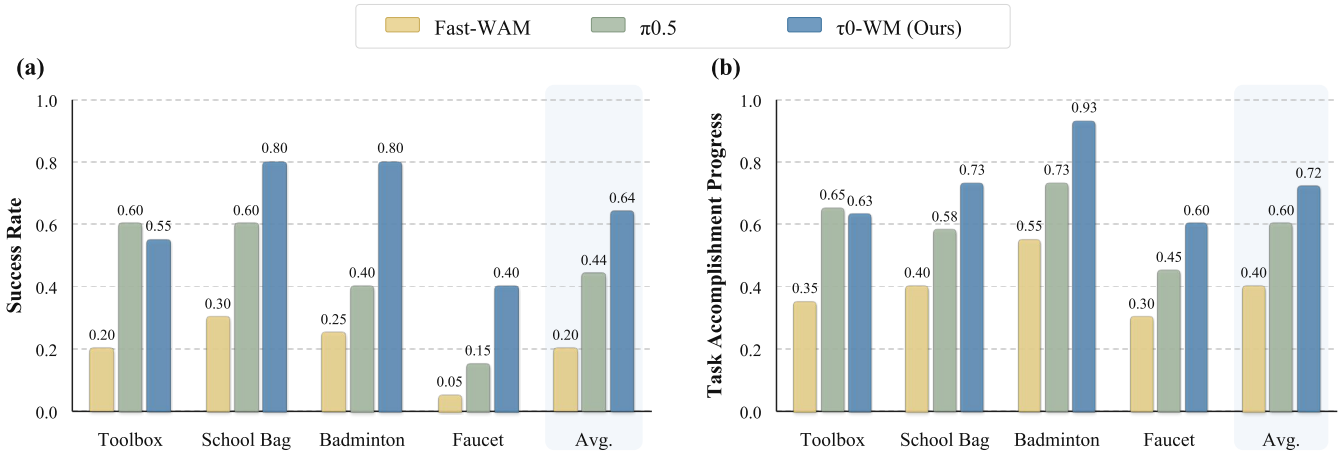

Fig. 4. **Comparison of different models in terms of success rate and task accomplishment progress.** Considering the complexity of the long-horizon tasks, we evaluate different models using both task success rate and stepwise task accomplishment progress.

TABLE I
EFFECT OF EGO AND UMI PRE-TRAINING. SUCCESS RATES ON ZERO-SHOT AND SFT EVALUATION FOR DIFFERENT PRETRAINING RECIPE.

Zero-shot: Pen-to-holder			
Data	Clean	Clut.	Avg.
Robot	0.22	0.06	0.14
Robot+UMI+Ego	**0.56**	**0.53**	**0.55**
SFT: Object-wipe-place			
Data	Clean	Clut.	Avg.
Robot	0.85	0.55	0.70
Robot+UMI+Ego	**0.90**	**0.75**	**0.83**

TABLE II
COMPARISON BETWEEN TEST-TIME COMPUTATION VARIANTS. SUCCESS RATE IS REPORTED FOR EACH TASK AND AVERAGED ACROSS TASKS. ONE-TIME COMPLETION ONLY. RETRIES ARE NOT ALLOWED.

Variant	Tissue→Box	Pen→Box	Avg.
w/o TTC	0.55	0.30	0.43
w. CFG [18]	0.25	0.15	0.20
w. ACG [32]	0.40	0.35	0.38
w. RCS	0.65	0.35	0.50
w. RCS + LAR	**0.70**	**0.50**	**0.60**

attachment. To evaluate embodiment diversity, *Badminton* is conducted on the ARX manipulator and *Faucet* on the dual-arm Franka platform, while the remaining tasks are performed on AGIBOT-G01.

Fig. 4 shows that τ_0-WM achieves the highest average success rate and performs best on most tasks. Although $\pi_{0.5}$ performs competitively on *Toolbox*, its performance degrades on tasks requiring longer-horizon coordination and fine-grained manipulation. In contrast, τ_0-WM remains consistently strong across all four tasks. Notably, *Faucet* remains challenging for every method, indicating that the task is far from saturated; nevertheless, τ_0-WM achieves the highest success rate under these strict alignment constraints. We attribute this advantage to the joint modeling of future visual dynamics and executable actions, which provides richer predictive supervision than action-only policy learning. Overall, these results demonstrate that VAM scales effectively across multiple robot embodiments while maintaining strong long-horizon manipulation capability.

Interestingly, we also observe qualitative differences that are not captured by the binary success metric. In the *Toolbox* task, baseline policies frequently stop once a tool is inserted into the correct slot, even when the insertion is incomplete or the tool remains loosely positioned. By contrast, τ_0-WM often performs additional corrective actions, such as pushing or pressing the tool further into place, before terminating the episode. We hypothesize that this behavior emerges from the explicit modeling of future visual outcomes, which encourages the policy to optimize for the quality of the final scene configuration rather than merely reaching an intermediate task-completion state.

B. Ablation Studies

Pre-training data composition. To validate the effectiveness of the proposed pretraining data mixture, we trained two τ_0-WM models: a model trained exclusively on robot teleoperation data, and a model trained on the complete pretraining corpus. We conduct the comparison under both zero-shot execution and supervised fine-tuning. The zero-shot task requires picking up a pen and placing it into a pen holder, while the fine-tuning task requires picking up an object, wiping off dirt, and returning it to the tabletop. Both tasks are evaluated in clean and cluttered tabletop variants.

Table I shows that adding UMI and egocentric data improves performance in both settings. The gain is most pronounced in the zero-shot setting, where success rate improves from 0.14 to 0.55 on average. This suggests that UMI and egocentric interaction data primarily improve general-purpose manipulation priors and visual understanding, which transfer effectively to

previously unseen tasks. The benefit remains visible after SFT, particularly under cluttered conditions, indicating improved robustness rather than merely faster adaptation.

Test-time computation. We ablate the proposed test-time computation strategy on two tasks based on the pretrained VAM: pulling out a tissue and placing it into a box (*Tissue→Box*) and picking up a pen and placing it into a box (*Pen→Box*). To isolate the effect of TTC, we adopt a stricter protocol that allows only a single attempt without retries. Each experiment is repeated 20 times.

Unless otherwise specified, TTC uses four action proposals per decision step. It consists of two stages: *RCS*, which performs lightweight self-consistency-based candidate selection, and *LAR*, which invokes ACVS for rollout-based action rectification when the selected action is deemed unreliable.

Table II shows that both stages of the proposed test-time computation improve execution performance under the single-attempt setting. Using only the lightweight RCS filter increases the average success rate from 0.43 to 0.50, indicating that a substantial portion of failures originates from selecting suboptimal action samples rather than insufficient policy capability. Further enabling LAR improves the average success rate to 0.60 by leveraging action-conditioned future rollouts for action rectification.

Table II also compares our method with existing generation-time guidance approaches. While CFG [18] and ACG [32] modify the generation process itself, our approach explicitly evaluates candidate actions and their induced futures before execution. As a result, RCS+LAR consistently achieves the best performance across all tasks. The larger improvement on *Pen→Box* further suggests that future-conditioned rectification is particularly beneficial for manipulation tasks that require precise object placement and alignment.

VIII. Conclusion and Future Work

We presented τ_0-WM, a unified video-action world model that combines action generation, future prediction, and deployment-time reasoning within a single predictive framework.

A key aspect of τ_0-WM is its ability to learn from heterogeneous interaction data, including real-robot teleoperation, UMI-style demonstrations, egocentric human videos, and simulator-oriented rollout trajectories. This unified training paradigm enables video prediction and action generation to be learned within a single framework while supporting deployment-time reasoning. Experiments on long-horizon, fine-grained manipulation tasks demonstrate strong policy performance across multiple robot embodiments, consistent gains from heterogeneous pre-training, and significant improvements from test-time computation.

Looking forward, several directions remain promising. First, many dexterous manipulation tasks require information beyond vision alone. Incorporating additional sensing modalities, particularly tactile feedback, may enable more reliable modeling of contact-rich interactions such as insertion, fastening, and deformable object manipulation. Second, while the proposed test-time computation strategy already improves execution performance, developing more reliable deployment-time reasoning mechanisms remains an important challenge. Better uncertainty estimation, longer-horizon evaluation, and more effective search strategies may further improve action selection in difficult states. Finally, extending predictive modeling to longer temporal horizons and more complex manipulation scenarios may enable richer future imagination and stronger decision-making capabilities.

Overall, we believe predictive robot learning provides a promising path toward more capable and reliable robot foundation models, and τ_0-WM offers an practical step in this direction.

IX. Acknowledgement

We would like to thank Jinyu Zhang, Sen Wang, Youlun Peng, Xinlin Ren, Mingjie Pan, Jianheng Song, Siyuan Feng, Zhongyuan Liu, Dong Li, Xiaowei Cai, Dafeng Wei, Han Jiang, Runkun Ju, Shaowei Li, Li Wang Buqing Nie, Kefeng Tang for their valuable contributions and support throughout this project. Their efforts in data collection, system development, experiment deployment, infrastructure maintenance, and engineering implementation were essential to the completion of this work.

APPENDIX

A. Training and Deploymeny Details

1) Training Configuration: τ_0-WM is trained in two stages. The pre-training stage uses 27.3K hours of heterogeneous interaction data, including real-robot teleoperation, UMI-style interaction data, egocentric human videos, and rollout or failure trajectories. The post-training stage further adapts the model to downstream robotic manipulation tasks.

The pre-training and post-training stages use global batch sizes of 12,288 and 384, respectively. Both stages use the AdamW optimizer with a learning rate of 5×10^{-5}. Unless otherwise specified, all experiments use the same optimization hyperparameters across embodiments and tasks.

2) Deployment Details: All real-robot experiments are performed under language-conditioned multi-view observations. Unless otherwise stated, actions are executed in a receding-horizon closed-loop manner using fixed-length action chunks of 30.

Real-robot inference is deployed on a single RTX 5090 GPU. Under the standard deployment configuration, the end-to-end action generation latency is approximately 220 ms per query. By caching reusable text representations, the latency can be reduced to approximately 180 ms without changing model outputs.

B. Inference Acceleration

To improve deployment efficiency, we employ several implementation-level optimizations.

1) Cross-Attention KV Cache: During action-only inference, the video branch provides conditioning features for the action branch through cross-attention. Since the visual context remains unchanged throughout the denoising process, the corresponding key and value tensors are computed once and reused across all sampling steps.

Let $x^{(l)}$ denote the video feature at transformer layer l. We cache

$$K_v^{(l)} = W_K x^{(l)}, \qquad V_v^{(l)} = W_V x^{(l)}, \tag{12}$$

and reuse them throughout inference, eliminating redundant projection operations.

2) Fused QKV Projection: We fuse query, key, and value projections into a single matrix multiplication,

$$[Q, K, V] = W_{QKV} x, \tag{13}$$

which reduces kernel launch overhead and improves memory throughput compared with three independent projection layers.

3) Simplified Rotary Position Embedding: Action tokens form a one-dimensional temporal sequence. We therefore precompute one-dimensional rotary position embeddings and reuse them throughout deployment, avoiding repeated frequency construction and reducing positional encoding overhead.

4) Torch Compile Optimization: We additionally employ `torch.compile` [4] with per-block compilation. Combined with the optimizations above, deployment latency can be further reduced from approximately 180 ms to 140 ms. Although `torch.compile` generally preserves model functionality, compiler-level graph transformations and kernel fusion may introduce small numerical differences compared with eager execution. For diffusion-based models, such differences can occasionally propagate through the sampling process and lead to slightly different outputs. Therefore, unless otherwise specified, all results reported in the main paper are obtained without `torch.compile` to ensure consistency and reproducibility across experiments.

References

[1] Niket Agarwal, Arslan Ali, Maciej Bala, Yogesh Balaji, Erik Barker, Tiffany Cai, Prithvijit Chattopadhyay, Yongxin Chen, Yin Cui, Yifan Ding, et al. Cosmos world foundation model platform for physical ai. *arXiv preprint arXiv:2501.03575*, 2025.

[2] Arslan Ali, Junjie Bai, Maciej Bala, Yogesh Balaji, Aaron Blakeman, Tiffany Cai, Jiaxin Cao, Tianshi Cao, Elizabeth Cha, Yu-Wei Chao, et al. World simulation with video foundation models for physical ai. *arXiv preprint arXiv:2511.00062*, 2025.

[3] Eloi Alonso, Adam Jelley, Vincent Micheli, Anssi Kanervisto, Amos Storkey, Tim Pearce, and François Fleuret. Diffusion for world modeling: Visual details matter in atari. *Advances in Neural Information Processing Systems*, 37:58757–58791, 2024.

[4] Jason Ansel, Edward Yang, Horace He, Ozgur K. Ulyanov, et al. Pytorch 2: Faster machine learning through dynamic python bytecode transformation and graph compilation. In *Proceedings of the 29th ACM International Conference on Architectural Support for Programming Languages and Operating Systems (ASPLOS)*, 2024.

[5] Hongzhe Bi, Hengkai Tan, Shenghao Xie, Zeyuan Wang, Shuhe Huang, Haitian Liu, Ruowen Zhao, Yao Feng, Chendong Xiang, Yinze Rong, et al. Motus: A unified latent action world model. *arXiv preprint arXiv:2512.13030*, 2025.

[6] Kevin Black, Noah Brown, James Darpinian, Karan Dhabalia, Danny Driess, Adnan Esmail, Michael Robert Equi, Chelsea Finn, Niccolo Fusai, Manuel Y Galliker, et al. $\pi_{0.5}$: a vision-language-action model with open-world generalization. In *9th Annual Conference on Robot Learning*, 2025.

[7] Tim Brooks, Bill Peebles, Connor Holmes, Will DePue, Yufei Guo, Li Jing, David Schnurr, Joe Taylor, Troy Luhman, Eric Luhman, Clarence Wing Yin Ng, Ricky Wang, and Aditya Ramesh. Video generation models as world simulators. https://openai.com/research/video-generation-models-as-world-simulators, 2024. OpenAI research blog.

[8] Chang Chen, Yi-Fu Wu, Jaesik Yoon, and Sungjin Ahn. Transdreamer: Reinforcement learning with transformer world models. *arXiv preprint arXiv:2202.09481*, 2022.

[9] Cheng Chi, Zhenjia Xu, Chuer Pan, Eric Cousineau, Benjamin Burchfiel, Siyuan Feng, Russ Tedrake, and Shuran Song. Universal manipulation interface: In-the-wild robot teaching without in-the-wild robots. *arXiv preprint arXiv:2402.10329*, 2024.

[10] Frederik Ebert, Chelsea Finn, Sudeep Dasari, Annie Xie, Alex Lee, and Sergey Levine. Visual foresight: Model-based deep reinforcement learning for vision-based robotic control. *arXiv preprint arXiv:1812.00568*, 2018.

[11] Chelsea Finn and Sergey Levine. Deep visual foresight for planning robot motion. In *2017 IEEE international conference on robotics and automation (ICRA)*, pages 2786–2793. IEEE, 2017.

[12] Shenyuan Gao, William Liang, Kaiyuan Zheng, Ayaan Malik, Seonghyeon Ye, Sihyun Yu, Wei-Cheng Tseng, Yuzhu Dong, Kaichun Mo, Chen-Hsuan Lin, et al. Dreamdojo: A generalist robot world model from large-scale human videos. *arXiv preprint arXiv:2602.06949*, 2026.

[13] GenRobot. 10kh realomni-open dataset. https://www.genrobot.ai/data/open-dataset, 2025. 1M+ clips from real-world and omni-scene robotic manipulation.

[14] Google DeepMind. Veo: A video generation system. https://deepmind.google/technologies/veo/, 2024.

[15] Yanjiang Guo, Lucy Xiaoyang Shi, Jianyu Chen, and Chelsea Finn. Ctrl-world: A controllable generative world model for robot manipulation. *arXiv preprint arXiv:2510.10125*, 2025.

[16] Yoav HaCohen, Nisan Chiprut, Benny Brazowski, Daniel Shalem, Dudu Moshe, Eitan Richardson, Eran Levin, Guy Shiran, Nir Zabari, Ori Gordon, et al. Ltx-video: Realtime video latent diffusion. *arXiv preprint arXiv:2501.00103*, 2024.

[17] Danijar Hafner, Timothy Lillicrap, Jimmy Ba, and Mohammad Norouzi. Dream to control: Learning behaviors by latent imagination. *arXiv preprint arXiv:1912.01603*, 2019.

[18] Jonathan Ho and Tim Salimans. Classifier-free diffusion guidance. *arXiv preprint arXiv:2207.12598*, 2022.

[19] Ryan Hoque, Peide Huang, David J Yoon, Mouli Sivapurapu, and Jian Zhang. Egodex: Learning dexterous manipulation from large-scale egocentric video. *arXiv preprint arXiv:2505.11709*, 2025.

[20] Siyuan Huang, Liliang Chen, Pengfei Zhou, Shengcong Chen, Yue Liao, Zhengkai Jiang, Yue Hu, Peng Gao, Hongsheng Li, Maoqing Yao, et al. Enerverse: Envisioning embodied future space for robotics manipulation. *Advances in Neural Information Processing Systems*, 38: 37693–37720, 2026.

[21] Yuxin Jiang, Shengcong Chen, Siyuan Huang, Liliang Chen, Pengfei Zhou, Yue Liao, Xindong He, Chiming Liu, Hongsheng Li, Maoqing Yao, et al. Enerverse-ac: Envisioning embodied environments with action condition. *arXiv preprint arXiv:2505.09723*, 2025.

[22] R.E. Kalman. A new approach to linear filtering and prediction problems. *Journal of Basic Engineering*, 82 (1):35–45, 1960.

[23] Alexander Khazatsky, Karl Pertsch, Suraj Nair, Ashwin Balakrishna, Sudeep Dasari, Siddharth Karamcheti, Soroush Nasiriany, Mohan Kumar Srirama, Lawrence Yunliang Chen, Kirsty Ellis, et al. Droid: A large-scale in-the-wild robot manipulation dataset. *arXiv preprint arXiv:2403.12945*, 2024.

[24] Moo Jin Kim, Yihuai Gao, Tsung-Yi Lin, Yen-Chen Lin, Yunhao Ge, Grace Lam, Percy Liang, Shuran Song, Ming-Yu Liu, Chelsea Finn, et al. Cosmos policy: Fine-

tuning video models for visuomotor control and planning. *arXiv preprint arXiv:2601.16163*, 2026.

[25] Weijie Kong, Qi Tian, Zijian Zhang, Rox Min, Zuozhuo Dai, Jin Zhou, Jiangfeng Xiong, Xin Li, Bo Wu, Jianwei Zhang, et al. Hunyuanvideo: A systematic framework for large video generative models. *arXiv preprint arXiv:2412.03603*, 2024.

[26] Lin Li, Qihang Zhang, Yiming Luo, Shuai Yang, Ruilin Wang, Fei Han, Mingrui Yu, Zelin Gao, Nan Xue, Xing Zhu, et al. Causal world modeling for robot control. *arXiv preprint arXiv:2601.21998*, 2026.

[27] Shuang Li, Yihuai Gao, Dorsa Sadigh, and Shuran Song. Unified video action model. *arXiv preprint arXiv:2503.00200*, 2025.

[28] Junbang Liang, Pavel Tokmakov, Ruoshi Liu, Sruthi Sudhakar, Paarth Shah, Rares Ambrus, and Carl Vondrick. Video generators are robot policies. *arXiv preprint arXiv:2508.00795*, 2025.

[29] Yue Liao, Pengfei Zhou, Siyuan Huang, Donglin Yang, Shengcong Chen, Yuxin Jiang, Yue Hu, Jingbin Cai, Si Liu, Jianlan Luo, et al. Genie envisioner: A unified world foundation platform for robotic manipulation. *arXiv preprint arXiv:2508.05635*, 2025.

[30] Yaron Lipman, Ricky TQ Chen, Heli Ben-Hamu, Maximilian Nickel, and Matt Le. Flow matching for generative modeling. In *11th International Conference on Learning Representations, ICLR 2023*, 2023.

[31] Abby O'Neill, Abdul Rehman, Abhiram Maddukuri, Abhishek Gupta, Abhishek Padalkar, Abraham Lee, Acorn Pooley, Agrim Gupta, Ajay Mandlekar, Ajinkya Jain, et al. Open x-embodiment: Robotic learning datasets and rt-x models: Open x-embodiment collaboration 0. In *2024 IEEE International Conference on Robotics and Automation (ICRA)*, pages 6892–6903. IEEE, 2024.

[32] Minho Park, Kinam Kim, Junha Hyung, Hyojin Jang, Hoiyeong Jin, Jooyeol Yun, Hojoon Lee, and Jaegul Choo. Acg: Action coherence guidance for flow-based vla models. *arXiv preprint arXiv:2510.22201*, 2025.

[33] William Peebles and Saining Xie. Scalable diffusion models with transformers. In *Proceedings of the IEEE/CVF international conference on computer vision*, pages 4195–4205, 2023.

[34] Adam Polyak, Amit Zohar, Andrew Brown, Andros Tjandra, Animesh Sinha, Ann Lee, Apoorv Vyas, Bowen Shi, Chih-Yao Ma, Ching-Yao Chuang, et al. Movie gen: A cast of media foundation models. *arXiv preprint arXiv:2410.13720*, 2024.

[35] Ryan Punamiya, Simar Kareer, Zeyi Liu, Josh Citron, Ri-Zhao Qiu, Xiongyi Cai, Alexey Gavryushin, Jiaqi Chen, Davide Liconti, Lawrence Y Zhu, et al. Egoverse: An egocentric human dataset for robot learning from around the world. *arXiv preprint arXiv:2604.07607*, 2026.

[36] Ropedia. Xperience-10m: A large-scale egocentric multimodal dataset with structured 3d/4d annotations, 2026. Dataset.

[37] Runway. Runway gen-4: Ai video generation with world consistency. https://runwayml.com/research/introducing-runway-gen-4, 2025.

[38] Homer Rich Walke, Kevin Black, Tony Z Zhao, Quan Vuong, Chongyi Zheng, Philippe Hansen-Estruch, Andre Wang He, Vivek Myers, Moo Jin Kim, Max Du, et al. Bridgedata v2: A dataset for robot learning at scale. In *Conference on Robot Learning*, pages 1723–1736. PMLR, 2023.

[39] Team Wan, Ang Wang, Baole Ai, Bin Wen, Chaojie Mao, Chen-Wei Xie, Di Chen, Feiwu Yu, Haiming Zhao, Jianxiao Yang, et al. Wan: Open and advanced large-scale video generative models. *arXiv preprint arXiv:2503.20314*, 2025.

[40] Philipp Wu, Alejandro Escontrela, Danijar Hafner, Pieter Abbeel, and Ken Goldberg. Daydreamer: World models for physical robot learning. In *Conference on robot learning*, pages 2226–2240. PMLR, 2023.

[41] Sherry Yang, Yilun Du, Kamyar Ghasemipour, Jonathan Tompson, Leslie Pack Kaelbling, Dale Schuurmans, and Pieter Abbeel. Learning interactive real-world simulators. *arXiv preprint arXiv:2310.06114*, 2023.

[42] Zhuoyi Yang, Jiayan Teng, Wendi Zheng, Ming Ding, Shiyu Huang, Jiazheng Xu, Yuanming Yang, Wenyi Hong, Xiaohan Zhang, Guanyu Feng, et al. Cogvideox: Text-to-video diffusion models with an expert transformer. In *International Conference on Learning Representations*, volume 2025, pages 83048–83077, 2025.

[43] Angen Ye, Boyuan Wang, Chaojun Ni, Guan Huang, Guosheng Zhao, Hao Li, Hengtao Li, Jie Li, Jindi Lv, Jingyu Liu, et al. Gigaworld-policy: An efficient action-centered world–action model. *arXiv preprint arXiv:2603.17240*, 2026.

[44] Seonghyeon Ye, Yunhao Ge, Kaiyuan Zheng, Shenyuan Gao, Sihyun Yu, George Kurian, Suneel Indupuru, You Liang Tan, Chuning Zhu, Jiannan Xiang, et al. World action models are zero-shot policies. *arXiv preprint arXiv:2602.15922*, 2026.

[45] Tianyuan Yuan, Zibin Dong, Yicheng Liu, and Hang Zhao. Fast-wam: Do world action models need test-time future imagination? *arXiv preprint arXiv:2603.16666*, 2026.

[46] Chuning Zhu, Raymond Yu, Siyuan Feng, Benjamin Burchfiel, Paarth Shah, and Abhishek Gupta. Unified world models: Coupling video and action diffusion for pretraining on large robotic datasets. *arXiv preprint arXiv:2504.02792*, 2025.